Planta (2002) 215: 33–40
DOI 10.1007/s00425-001-0718-9

ORIGINAL ARTICLE

Lothar Köhler · Hanns-Christof Spatz

Micromechanics of plant tissues beyond the linear-elastic range

Received: 1 August 2001 / Accepted: 3 November 2001 / Published online: 6 February 2002

Abstract We investigated the relation between cell wall structure and the resulting mechanical characteristics of different plant tissues. Special attention was paid to the mechanical behaviour beyond the linear-elastic range, the underlying micromechanical processes and the fracture characteristics. The previously proposed model of reorientation and slippage of the cellulose microfibrils in the cell wall [H.-CH. Spatz et al. (1999) J Exp Biol 202:3269–3272) was supported and is here refined, using measurements of the changes in microfibrillar angle during straining. Our model explains the widespread phenomenon of stress-strain curves with two linear portions of different slope and sheds light on the micromechanical processes involved in viscoelasticity and plastic yield. We also analysed the velocity dependence of viscoelasticity under the perspective of the Kelvin model, resolving the measured viscoelasticity into functions of a velocity-dependent and a velocity-independent friction. The influence of lignin on the above-mentioned mechanical properties was examined by chemical lignin extraction from tissues of *Aristolochia macrophylla* Lam. and by the use of transgenic plants of *Arabidopsis thaliana* (L.) Heynh. with reduced lignin content. Additionally, the influence of extraction of hemicelluloses on the mechanical properties was investigated as well as a cell wall mutant of *Arabidopsis* with an altered configuration of the cellulose microfibrils.

Keywords *Arabidopsis* (micromechanics) · *Aristolochia* (micromechanics) · Cellulose microfibril orientation · Fracture surface · Lignin · X-ray scattering

L. Köhler (✉) · H.-C. Spatz
Plant Biomechanics Group, Institut für Biologie III,
Universität Freiburg, Schänzlestrasse 1,
79104 Freiburg, Germany
E-mail: mail@lhkoehler.de
Fax: +49-761-203 2745

Introduction

Investigations into the mechanical properties of biological materials mostly deal with the initial linear-elastic range of the material's response to the given mode of loading – be it bending, straining, compression or shear. Additionally, factors like breaking strain or breaking stress are often considered, which for example in the case of trees is of vital interest with respect to safety factors (Niklas 2000). The range beyond the linear-elastic response and below ultimate failure is generally designated as 'yield' and rarely further investigated.

Since changes in form or structure of the material take place in the range beyond linear-elastic behaviour, a closer look at it is worthwhile. Moreover, some questions explicitly demand such knowledge over the whole range of the material's response to loading (Vincent 1975; Koehl and Wainwright 1977; Spatz et al. 1998; Beismann et al. 2000). A widely observed phenomenon at loading in tension beyond the linear-elastic range is the transition to a second linear section of smaller slope than that of the initial part. This is observed for biological materials such as animal membranes (Vincent 1975), tendons (Torp et al. 1975) or wood (Page et al. 1971; Bodig and Jane 1993), but is not limited to biological tissues: it is also found for synthetic composite materials (Schaffer 1964) and polycrystals (Ashby and Jones 1996). Naturally, the mechanisms responsible for this phenomenon vary since these materials differ substantially in their structure. Here, we invest3igate the phenomenon of 'biphasic' stress-strain curves for sclerenchyma isolated from *Aristolochia macrophylla* as an example of woody tissues. Our previously developed model treats such tissues as composite materials with cellulose microfibrils as fibres and a matrix consisting predominantly of hemicelluloses and lignin. The applied load is transferred into the fibres by shear forces at the interface to the matrix. Because of the different moduli of elasticity of fibres and matrix, shear forces build up between these two components. Above a certain strain

the matrix undergoes plastic deformation and the fibres can slide past one another (Spatz et al. 1999). This is confirmed here in further quantitative analyses, including the measurement of the changes in angular inclination of the cellulose microfibrils upon straining. Also, scanning electron microscopy of fracture surfaces allows conclusions about the micromechanical processes taking place beyond elasticity. The model explains the characteristic response to repeated loading-unloading cycles and sheds light on viscoelastic behaviour and the role of individual cell-wall components. The latter aspect was amplified by measurements on tissues with chemically or genetically altered cell wall matrix composition.

Materials and methods

Materials

Aristolochia macrophylla Lam. was obtained from the outdoor plantings of the Botanical Garden Freiburg. The sections used were less than 1 year old but fully differentiated. The axis diameter was 5–6 mm (compare with Fig. 2 in Köhler et al. 2000). The sclerenchyma tissue was prepared from the longitudinally dissected axes by removing the surrounding soft tissues. All samples were kept moist and cool for no longer than 1 day before use. *Arabidopsis thaliana* (L.) Heynh., ecotype Wassilewskija was grown in a 16 h:8 h white-light:dark cycle at a photon flux density of 50 μmol m^{-2} s^{-1}. The seeds of the wild type and the mutants were provided by the Laboratoire de Biologie Cellulaire, INRA, Versaille, France. The measurements on *Arabidopsis* were all done with sections of fresh entire shoots. For details about the mutant *botero* (*bot1-7*) see Bichet et al. (2001). In the mutant *asccr2.7* the expression of cinnamoyl-CoA reductase, an enzyme involved in lignin synthesis, is reduced to about 20% of the amount found in the wild-type plant. This results in a reduced lignin content of 54% of the wild type (L. Jouanin, INRA, Versaille, France, personal communication).

Mechanical tests

Tensile tests on sclerenchyma strips of *Aristolochia* or entire axis of *Arabidopsis* were carried out on an INSTRON Universal Testing Machine with strain rates around 5×10^{-4} s^{-1} if not otherwise stated. Samples were 3–5 cm in length and the sclerenchyma strips were about 1 mm in width and 0.2 mm thick.

Scanning electron microscopy

Fracture surfaces were pictured with a LEO 435 VP scanning electron microscope at 15 kV after air drying for 1 day and gold coating; for details see Spatz et al. (1999).

X-ray scattering

The average angular inclination of the cellulose microfibrils in the cell walls was determined by X-ray scattering (Preston 1952). This technique requires virtually no sample preparation and allows simultaneous straining of the sample. The results are inherently averaged over the structures inside the macroscopic sample volume covered by the X-ray beam. The experimental setup consists of a 6-kW rotating Cu-anode X-ray generator (Schneider, Offenburg, Germany). The incoming beam has a circular cross-section of 0.6 mm in diameter. The radiation wavelength is 0.154 nm, corresponding to CuKα radiation in combination with an Ni filter. The spectra were recorded on an image plate system with a sample-to-detector distance of 18 cm. As shown for wood by Jakob et al. (1994) the optimal sample thickness to avoid multiple scattering is around 0.2 mm, which in our case corresponds to the thickness of the sclerenchyma strips and rendered further preparation unnecessary. A Mini-Instron (Minimat 2000; Rheometric Scientific, Piscataway, N.J., USA) was employed for straining the samples. These were kept wet during the whole process of straining and X-ray measurement. The X-ray exposure time was 400 s. After each straining step the samples were allowed to settle for 400 s before the start of X-ray exposure. The microfibrillar angle was determined manually with an accuracy of $\pm 1°$ from radial intensity scans of the X-ray diagrams, plotted against the angular position.

Lignin quantification

The lignin contents of native and chemically altered tissue samples were determined by thioglycolic acid derivatisation and spectroscopic quantification according to Müsel et al. (1997).

Chemical extraction of lignin and hemicelluloses

Lignin was extracted oxidatively with an acetous solution of $NaClO_2$ (35–40 °C, 40 h); for details see Klauditz (1957). The hemicelluloses were degraded for 3 h by 2 M trifluoroacetic acid at 100 °C (Mankarios et al. 1979).

Results

Axes of *Aristolochia macrophylla* showed a typical biphasic behaviour when loaded in tension. This applied to the whole axis as well as to isolated tissue complexes and isolated tissues (Fig. 1). The corresponding stress-strain curves had two linear portions with a transition range in between. Most remarkable was the extended linear range at high strains almost up to the breaking strain (Fig. 2). Upon loading and unloading, viscoelasticity was observed as well as plastic deformation. In successive cycles on isolated sclerenchyma almost no further plastic deformation was found and viscoelastic behaviour dominated (Fig. 3). The overall energy loss is shown in Fig. 4. The high value for the first cycle results from the plastic yield processes in addition to the viscoelasticity. For subsequent cycles, the values differed only slightly and the viscoelasticity can be regarded as a nearly constant material property. In Fig. 5 the amount of viscoelasticity at different strain rates is shown. The values pass through a maximum and decline for high and low strain rates. This resembles the behaviour of a Kelvin element (insert to Fig. 5). The theoretical amount of damping according to this model is represented in Fig. 5 by the dashed line. The curve differs from the experimental data by a constant, i.e. a velocity-independent amount of friction. This shows that the viscoelasticity observed in this tissue is due to two different underlying types of friction – the so called Coulomb or dry friction which is independent of the velocity and the Stokes or viscous friction which increases linearly with speed and results in an overall damping behaviour that runs through a maximum. In the speed range investigated here, the loss of energy due to viscous friction amounted to 4–37% of the total energy loss.

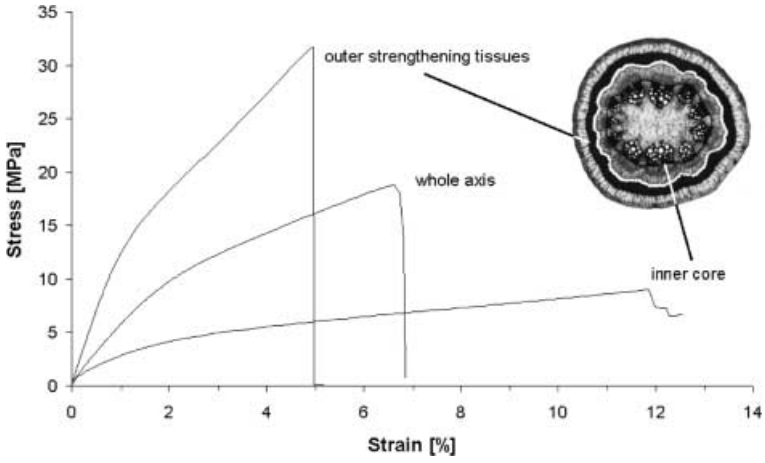

Fig. 1 Stress-strain curves of a young axis of *Aristolochia macrophylla* as a whole and separated into an outer ring of strengthening tissues and an inner core. The outer ring comprises collenchyma, parenchyma and sclerenchyma; the core comprises phloem, xylem bundles, interfascicular parenchyma and pith

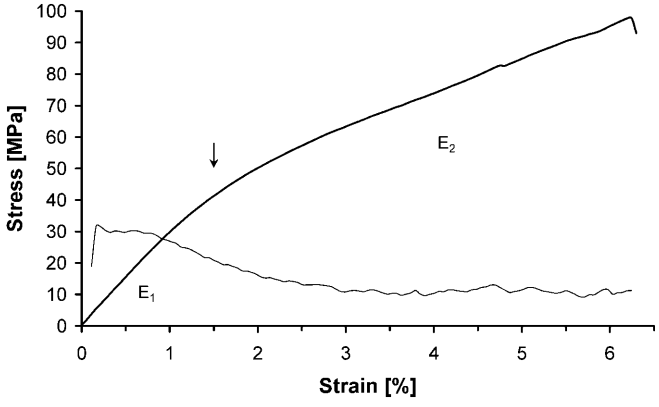

Fig. 2 Stress-strain curve (*bold line*) of isolated sclerenchyma tissue of *A. macrophylla*. The *arrow* marks the center of the transition region (''transition point'') between the two portions of the curve. *E1* Modulus of elasticity of the first portion of the stress-strain curve, *E2* modulus of elasticity of the second linear portion. The slope of the stress-strain curve (*thin line*) has two nearly constant regions, justifying the choice of the two moduli E1 and E2

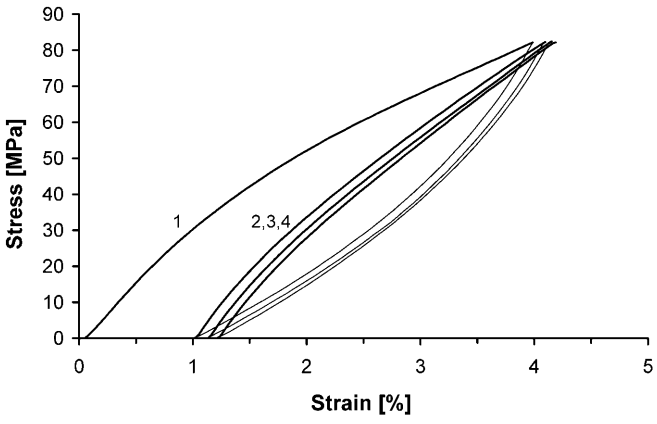

Fig. 3 Successive loading-unloading cycles on isolated sclerenchyma tissue of *A. macrophylla*. The numbers (*1–4*) indicate the successive cycles

Cyclic loading and unloading at strains beyond the transition point led to values of viscoelasticity more than three times higher than cycling below it (see Table 1). Together with the fact that there are two distinctly different moduli of elasticity for each of the two portions of the stress-strain curve, this suggests that the underlying micromechanical processes differ for each of the respective portions.

To elucidate the role of the cellulose microfibrils and their angular inclination with respect to the longitudinal axis of the cells we recorded the microfibrillar angle by X-ray scattering measurements as a function of the applied strain. An example of the X-ray measurements is shown in Fig. 6; the measured angles plotted against the relative extension of the samples are shown in Fig. 7. It can be seen that the inclination of the microfibrils decreased in the strain range below the transition point and remained roughly constant beyond it. After relaxing the samples to zero stress a residual deformation of $0.4 \pm 0.1\%$ remained and a microfibrillar angle of $16.5 \pm 1.1°$ (compared with an initial value of 16.0°) was observed.

In regard to the role of the cell wall matrix in the mechanical behaviour we investigated the influence of lignin and hemicelluloses. The mechanical relevance of lignin can already be seen in ontogenetical studies where a concurrent increase in lignin content and modulus of elasticity was observed at least up to a lignin content of 10% (Fig. 8). Naturally, this increase in stiffness is caused in part by the general increase in cell wall thickness, but for *Aristolochia macrophylla* this amounted to only a factor of 8 during the first year while the stiffness increased during the same time by a factor of 100. So qualitative modifications like lignification must play an important role (Köhler 2001).

By reducing the lignin content chemically, we could investigate its mechanical effect from a different perspective. Lignin content in the cell wall material was reduced by an average of 92% relative to the untreated samples. The qualitative changes in the stress-strain curve are exemplified along with the results from a hemicellulose-extracted sample in Fig. 9. A numerical overview is given in Table 1. The lignin-extracted tissue showed reduced moduli of elasticity E1 and E2 and the second phase of the cycle was brought to an upward non-linear closure. Yet the biphasic character was

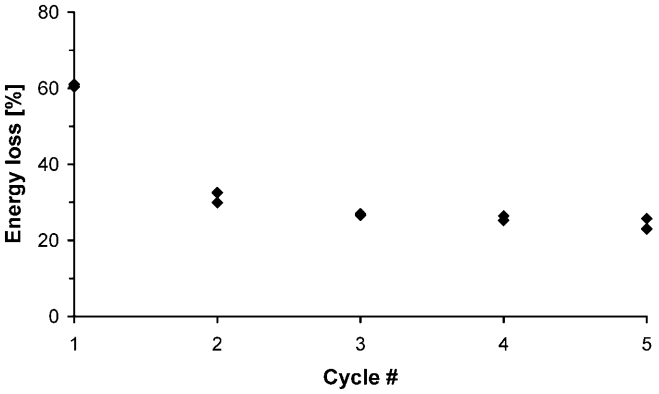

Fig. 4 Energy loss per cycle in loading-unloading experiments on isolated sclerenchyma tissue of *A. macrophylla* in the strain-range between 1.8 and 3.8% strain. The strain rate is 5×10^{-4} s^{-1}

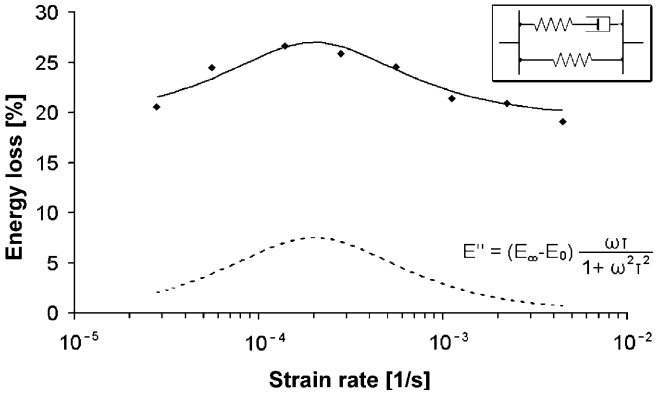

Fig. 5 Energy loss of isolated sclerenchyma tissue of *A. macrophylla* at different velocities of cycling, measured between 1.8 and 3.8% strain after two precursory cycles (*closed squares*). Energy loss according to the Kelvin model (*dashed line*). Results according to the model increased by an additive constant of 19.5 (*solid line*). The *insert* depicts the Kelvin model with springs and a dashpot

basically retained. Extraction of hemicelluloses resulted in a reduction in the initial modulus of elasticity and in fracture at an extension where in the untreated case the transition point is situated. No second phase was observed here. The mechanical behaviour in the dry state is exemplified in Fig. 10. In all cases the modulus of elasticity increased upon drying. For the de-lignified and the hemicellulose-extracted tissues it increased much more strongly than in the untreated case. So in the dried state the modulus of elasticity did not differ appreciably for the untreated and the de-lignified samples, which is consistent with the supposition that the main impact of lignin on the mechanical properties is due to its hydrophobicity and is thus particularly relevant in the moist state.

Since the possibility of artefacts introduced by the severe chemical treatment cannot be excluded, we also examined cell wall mutants of *Arabidopsis thaliana*. Although the mechanical properties of *A. thaliana* differed from those of *Aristolochia macrophylla*, the characteristic biphasic stress-strain behaviour was similar albeit less distinct (Fig. 11). In the mutant *asccr2.7*, the synthesis of lignin is altered, resulting in a lignin reduction of 54% compared to the wild type. *Botero* is a cytoskeleton mutant, in which the function of the cortical microtubules is impaired, with a consequent effect on the length or orientation of the cellulose microfibrils. Table 2 summarises our measurements of *Arabidopsis*. Comparison between the wild type and the *asccr2.7 A. thaliana* mutant showed similar trends to a comparison between untreated and chemically treated *Aristolochia* tissue. In both cases, the biphasic behaviour was conserved despite lignin reduction. Moreover, the transition between the two linear portions of the stress-strain curve remained practically unaltered with respect to the strain range. Yet, upon reduction of the lignin content stiffness decreased as reflected in a decrease in the moduli of elasticity (Table 2) and a lower stress level at the transition point. The large standard deviation results from the fact that the curves in the second phase are not as linear as for *Aristolochia*. Determinations of the transition point and the modulus of elasticity E2 in the second phase are therefore somewhat ambiguous.

As shown previously (Spatz et al. 1999; Beismann et al. 2000) the character of the fracture surface is an indication of the micromechanical processes taking place during straining. We investigated the mechanical behaviour and the fracture characteristics of wet and dry tissues in the untreated and chemically processed state. The striking difference in the character of the fracture surface between wet lignified and de-lignified samples disappeared in the dry state (compare also Figs. 9 and 10). As pointed out above this is not unexpected since lignin, through its hydrophobicity, indirectly influences the mechanical properties of wet material more than those of dry material. Untreated *Aristolochia* in the wet state showed a rugged fracture surface (Fig. 12) with torn-out fibres typical of a partial detachment of fibres and matrix. In contrast the fracture surface of the untreated dry sample was more typical of a brittle

Table 1 Mechanical properties of untreated and chemically treated sclerenchyma tissue of *Aristolochia macrophylla*. E1 and E2 are defined as in Fig. 2. Mean values ± SD

	Native ($n=8$)	Lignin extracted ($n=8$)	Hemicelluloses extracted ($n=6$)
E1 [GPa]	3.8 ± 0.7	2.4 ± 0.6	2.3 ± 0.2
E2 [GPa]	1.2 ± 0.2	0.7 ± 0.2	–
Strain at transition point [%]	1.4 ± 0.2	1.1 ± 0.1	–
Breaking strain [%]	6.1 ± 1.3	7.3 ± 1.2	1.2 ± 0.2
Viscoelasticity phase I [%]	4.2 ± 1.7	14.7 ± 1.0	
Viscoelasticity phase II [%]	15.2 ± 1.0	19.6 ± 1.2	

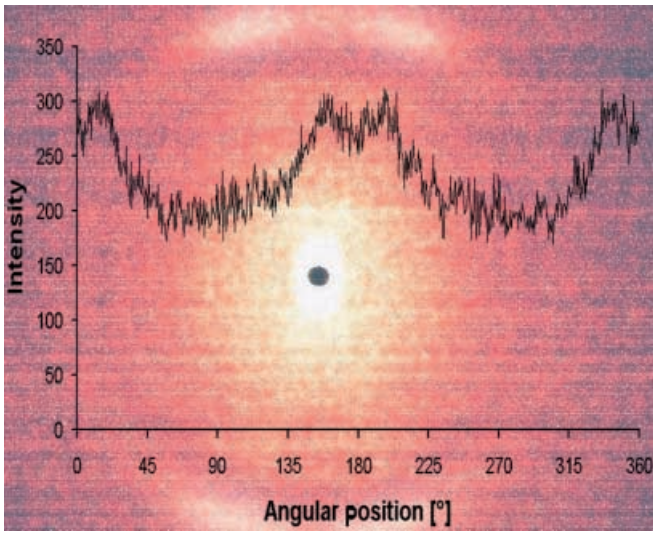

Fig. 6 Example of an X-ray scattering diagram for *A. macrophylla* sclerenchyma tissue and a radial intensity scan through the reflexes

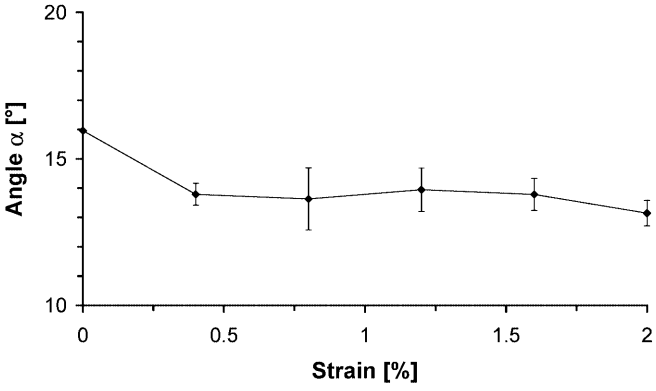

Fig. 7 The microfibrillar angle α of *A. macrophylla* as determined by X-ray scattering measurements on increasingly strained strips of sclerenchyma. The results of four independent measurements were normalised to the average value at zero strain. Error bars are standard deviations

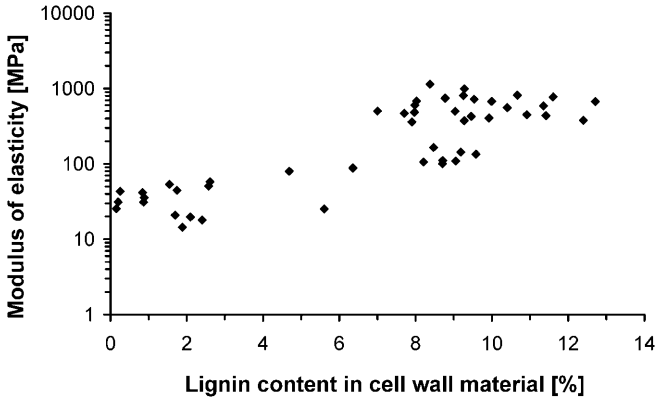

Fig. 8 Modulus of elasticity and lignin content of whole axes of *A. macrophylla* measured at different times during the first year of ontogeny

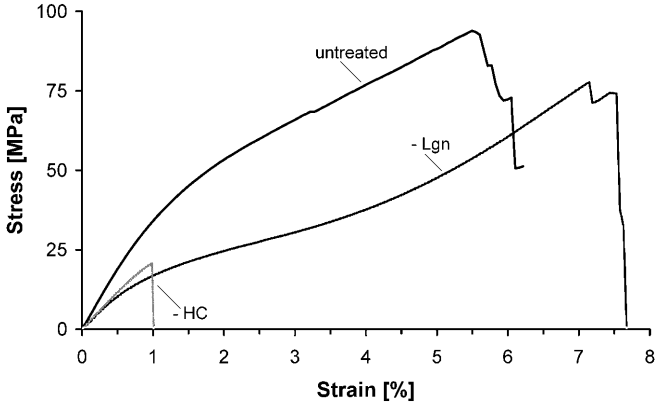

Fig. 9 Stress-strain curves of untreated and chemically treated wet sclerenchyma of *A. macrophylla*. *Lgn* De-lignified, *HC* hemicelluloses extracted

fracture. The de-lignified wet sample showed a fracture surface that was even rougher than that of the untreated wet state, while the fracture surface of the de-lignified dry sample was intermediate. The appearance of the wet hemicellulose extracted sample was different, since the fracture surface showed long torn-out fibres. This can also be seen in the dry hemicellulose-extracted sample, but to a much lesser degree.

Discussion

The mechanical properties of *Aristolochia macrophylla* have already been examined from an ontogenetical perspective (Köhler et al. 2000). Insights into the micromechanics could be derived from the ontogenetic changes in material and structure and the concurrent changes in the mechanical properties. However, since several factors change simultaneously during ontogeny, the precise cause-effect relationship between mechanical and structural changes remained problematic. Biological objects often experience mechanical loads straining them far beyond the linear-elastic range. In the present study, we measured changes in microfibrillar angle during extensive straining to elucidate the corresponding micromechanical processes. These investigations were complemented by studying the fracture surfaces and by comparing samples with genetically or chemically altered cell wall composition.

Biphasic stress-strain curves are found for many biological tissues, such as the watermoss *Fontinalis antipyretica* (Biehle et al. 1998), the horse-tail *Equisetum hyemale* (Spatz et al. 1998) and wood (Mark 1967). Using an elaborate experimental setup that permitted measurement of wood samples composed of only a few tracheids, Mark showed that biphasic stress-strain curves can reflect cell wall-level rather than tissue-level properties. Interpreting this in terms of composite materials, he adapted a theory of strain behaviour from synthetic composite materials (Shaffer 1964) that involves matrix yielding during the second linear portion

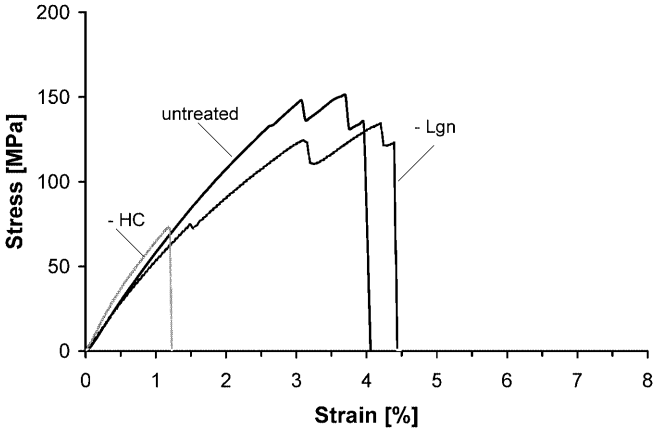

Fig. 10 Stress-strain curves of untreated and chemically treated dry sclerenchyma of *A. macrophylla*. *Lgn* De-lignified, *HC* hemicelluloses extracted

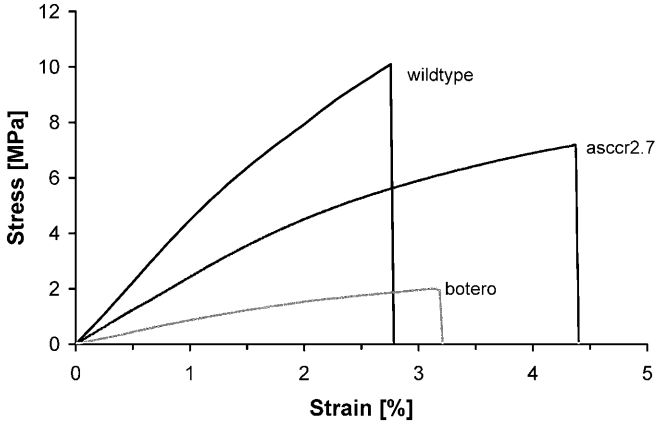

Fig. 11 Stress-strain curves of whole axes of wild-type and mutants of *Arabidopsis thaliana*

of the stress-strain curve. However the micromechanical processes as regards angle, reorientation, and slippage of the cellulose microfibrils were not studied. The potential relevance of slippage of the microfibrils past one another for the mechanical cell wall properties has been pointed out by Niklas (1992, p 246). Reiterer et al. (1998) examined the tensile properties of different kinds of wood as a function of the microfibrillar angle. Their results show linear to biphasic curves with different E1/E2 ratios depending on the microfibrillar orientation.

In accordance with these prior reports our results draw a consistent picture in regard to the micromechanical processes attending tissue extension. The mechanical behaviour of these matrix-fibre composite materials is determined by two processes: fibrillar reorientation and slippage due to yield of the matrix. Considering the changes in the microfibrillar angle during straining (Fig. 7), it is obvious that a significant change ($P < 0.001$) in microfibril orientation is taking place only during the first phase of the stress-strain curve, while during the second phase microfibril orientation remains approximately constant. Actually, the angular changes already cease before the strain of the transition point, as measured in continuous straining experiments (see Table 1), is reached. But this is consistent with the fact that for the X-ray measurements the straining had to be paused for about 8 min each time, during which yielding of the sample took place (reflected in a noticeable decay of the stress). The strains measured in these experiments therefore have to be corrected to higher values to be comparable to those measured in a continuous tension experiment. In addition, the inclination angle α is an average over a wide distribution of fibre angles. As explained below the relation between strain, fibrillar inclination and yield strain is non-linear, such that the yield point occurs at strains where the change in the average inclination angle is no longer noticeable.

Straining during the first phase causes no substantial plastic deformation after unloading while in the second phase it effects a residual plastic yield that increases linearly with increasing extension (see Köhler et al 2000). Upon unloading, the microfibrillar angle is reset to approximately the initial value despite the remaining plastic deformation.

This confirms our previous micromechanical model. The first portion of the biphasic stress-strain curve, exhibiting a high modulus of elasticity and little viscoelasticity, is due to elastic extension. The second portion is explained by yielding of the matrix and slippage of the microfibrils past each other. This leads to a decreased modulus of elasticity and a much higher viscoelasticity. The extension during the first phase causes the microfibrillar angle to decrease. The Poisson ratio of a helix with an inclination angle α is $1/tg^2\ \alpha$, while the Poisson ratio of a cell with constant volume is 0.5. Therefore if $\alpha < 54°$ the decrease in the inclination in helically arranged microfibrils goes along with a lateral compression of the cell (Mark 1967). This is only possible up to a certain degree and will then impede the microfibrils from further reorientation. Beyond this point the

Table 2 Mechanical properties of untreated and chemically treated sclerenchyma tissue of *Aristolochia macrophylla*. E1 and E2 are defined as in Fig. 2. Mean values ± SD

	Wild type ($n = 14$)	*Asccr2.7* ($n = 14$)	*Botero* ($n = 22$)
E1 [MPa]	379 ± 129	158 ± 61	69 ± 42
E2 [MPa]	198 ± 68	61 ± 50	23 ± 16
Strain at transition point [%]	1.6 ± 0.4	4.9 ± 1.7	4.3 ± 2.0
Breaking strain [%]	2.7 ± 0.7	4.9 ± 1.7	4.3 ± 2.0
Viscoelasticity phase I [%]	3.1 ± 1	9.4 ± 1	
Viscoelasticity phase II [%]	9.5 ± 0.5	13.0 ± 1	

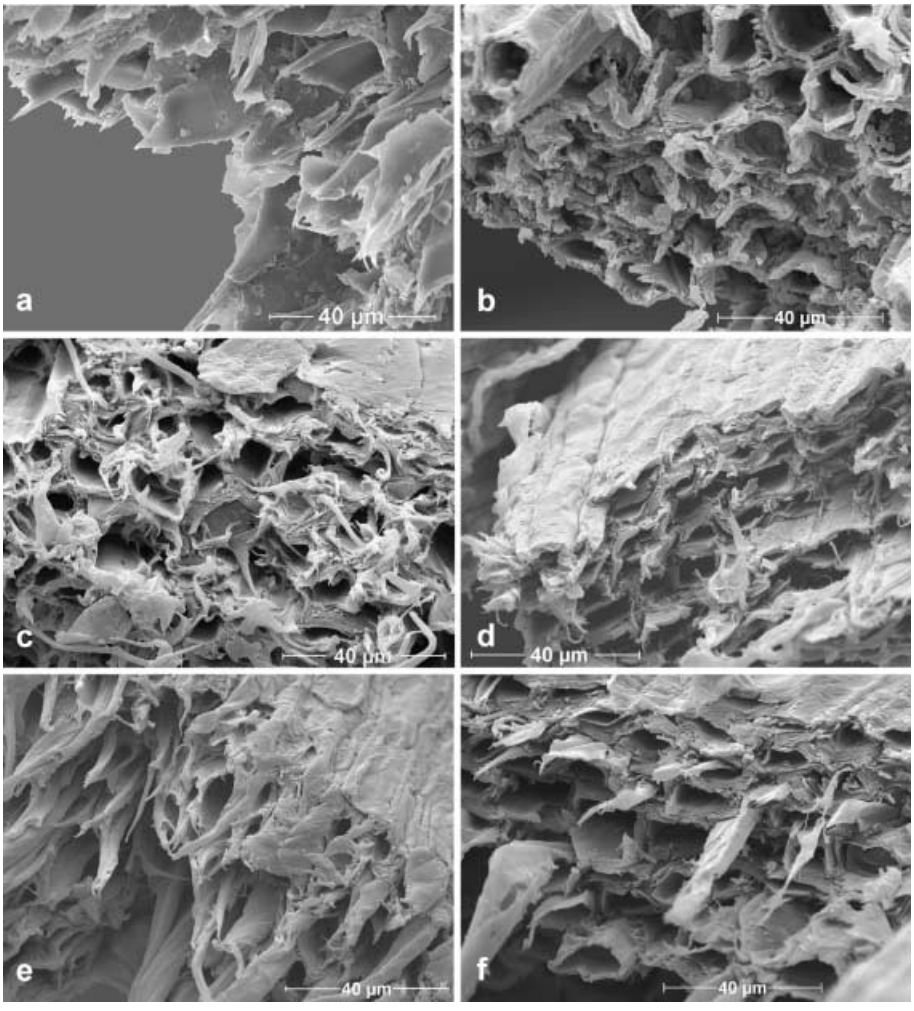

Fig. 12a–f Scanning electron microscope pictures of fracture surfaces of sclerenchyma tissue of *A. macrophylla*. **a** Untreated moist; **b** untreated dry; **c** de-lignified moist; **d** de-lignified dry; **e** hemicelluloses extracted, moist; **f** hemicelluloses extracted, dry

increase in length due to straining is provided by slippage of the microfibrils past each other and yield of the matrix.

A reduction in the lignin content reduces the moduli of elasticity (see Tables 1 and 2). Yet, despite the much higher reduction in lignin content in the case of the chemical extraction compared with the genetic modification, the relative decrease in the modulus of elasticity lies within the same range. This suggests that not all the lignin is mechanically relevant, so that the overall amount is not necessarily a direct indication of the mechanical properties. It is also consistent with ontogenetic studies showing that, beyond a certain lignin content, no further influence on the stiffness is noticeable (see Fig. 8 and Köhler et al. 2000). It is known that the highest lignin concentration is found in the middle lamella, whereas the concentration in the S2 layer is distinctly lower (Fengel 1983). As our pictures of the fracture surfaces of *Aristolochia* show, trans-wall fracture is the predominant mode of failure and not disintegration along cell-cell boundaries (see Fig. 12). So for these mechanical properties the middle lamella will not play an important role. This may explain why only a part of the overall lignin influences the mechanical behaviour.

It is also obvious that lignin is not substantially responsible for the biphasic shape. It basically "scales" the stress-strain curve but does not alter its general appearance. In the case of *Aristolochia* the breaking strain and the strain at the transition point are not significantly ($P < 0.2$) changed by de-lignification (see Table 1), only the respective stress is decreased. In the lignin-reduced mutant of *Arabidopsis* the breaking strain is increased and the transition point is shifted only marginally towards higher strains (see Table 2) but the biphasic character of the curve is conserved (see Fig. 11).

Further insight is provided by loading-unloading experiments. Viscoelasticity is increased by lignin reduction in the tissues of *Aristolochia* as well as in the lignin-reduced mutant of *Arabidopsis*. This higher inner friction indicates that the microfibrils are partially unlocked upon de-lignification and can move against each other, dissipating energy in this process.

In the case of the de-lignified samples of *Aristolochia* a new feature is found in the mechanical behaviour. At the end of the second phase of the stress-strain curve the stiffness increases continually with increasing strain. This phenomenon is well known for biological composites with random fibre distribution (Jeronimidis

and Vincent 1984). In our case, the cellulose microfibrils may have the ability to align more in the direction of the applied strain and in turn take up increasingly more load. Since the fibril orientation is in fact scattered around the mean value found in the X-ray measurements (see Köhler et al. 2000) it can be expected that some effects are normally obscured by the bulk behaviour if sufficient angular flexibility of the fibrils is provided.

The analysis of the material's behaviour at straining beyond the initial linear-elastic range thus delivers insights into the structural properties of the material and the dynamic interrelations between the different structural components.

Acknowledgement We thank H. Lichtenegger (Erich Schmidt Institut, Leoben, Austria) for her help and advice on the X-ray measurements as well as G. Strobl, B. Heck and Y. Men (Albert-Ludwig-Universität, Freiburg, Germany) for making the X-ray device available to us and for technical assistance. We are grateful to L. Jouanin and H. Hofte (INRA, Versaille, France) for providing seeds of the mutants of *Arabidopsis*, and to P. Schopfer (Albert-Ludwig-Universität, Freiburg, Germany) for putting his laboratory at our disposal for the lignin quantification. We also thank K. Niklas (Cornell University, Ithaca, USA) and B. Hoffmann (Albert-Ludwig-Universität, Freiburg, Germany) for critical comments on the manuscript. This work has been partly supported by the Ministerium für Wissenschaft, Forschung und Kunst Baden-Württemberg and DaimlerChrysler AG.

References

Ashby MF, Jones DRH (1969) Engineering materials 1: an introduction to their properties and applications. Butterworth Heinemann, Oxford

Beismann H, Wilhelmi H, Baillères H, Spatz H-CH, Bogenrieder A, Speck T (2000) Brittleness of twig bases in the genus *Salix*: fracture mechanics and ecological relevance. J Exp Bot 51:617–633

Bichet A, Desnos T, Turner S, Grandjean O, Höfte H (2001) *BOTERO1* is required for normal orientation of cortical microtubules and anisotropic cell expansion in *Arabidopsis*. Plant J 25:137–148

Biehle G, Speck T, Spatz H-CH (1998) Hydrodynamics and biomechanics of the submerged watermoss *Fontinalis antipyretica* – a comparison of specimens from habitats of different flow velocities. Bot Acta 111:42–50

Bodig J, Jayne BA (1993) Mechanics of wood and wood composites. Krieger Publishing Company, Malabar, Florida

Jakob HF, Fratzl P, Tschegg SE (1994) Size and arrangement of elementary cellulose fibrils in wood cells: a small-angle X-ray scattering study of *Picea abies*. J Struct Biol 113:13–22

Jeronimidis G, Vincent JFV (1984) Composite materials. In: Hukins DWL (ed) Connective tissue matrix. Verlag Chemie, Weinheim Deerfield Beach Florida

Fengel D (1983) Wood: chemistry, ultrastructure, reactions. DeGruyter, Berlin

Klauditz W (1957) Zur biologisch-mechanischen Wirkung der Cellulose und Hemicellulose im Festigungsgewebe der Laubhölzer. Holzforschung 11:110–116

Koehl MAR, Wainwright SA (1977) Mechanical adaptations of a giant kelp. Limnol Oceanogr 22:1067–1071

Köhler L, Speck T, Spatz H-CH (2000) Micromechanics and anatomical changes during early ontogeny of two lianescent *Aristolochia* species. Planta 210:691–700

Köhler L (2001) Mikromechanik von Pflanzengeweben jenseits des linear-elastischen Verhaltens. PhD thesis, Universität Freiburg, Germany

Mankarios AT, Jones CFG, Jarvis MC, Threlfall DR, Friend J (1979) Hydrolysis of plant polysaccharides and GLC analysis of their constituent neutral sugars. Phytochemistry 18:419–422

Mark E (1967) Cell wall mechanics of tracheids. Yale University Press, New Haven

Müsel G, Schindler T, Bergfeld R, Ruel K, Jacquet G, Lapierre C, Speth V, Schopfer P (1997) Structure and distribution of lignin in primary and secondary cell walls of maize coleoptiles analysed by chemical and immunological probes. Planta 201:146–159

Niklas KJ (1992) Plant Biomechanics. University of Chicago Press, Chicago London

Niklas KJ (2000) Computing factors of safety against wind-induced tree stem damage. J Exp Bot 51:797–806

Page DH, El-Hosseiny F, Winkler K (1971) Behaviour of single wood fibres under axial tensile strain. Nature 229:252–253

Preston RD (1952) The molecular architecture of plant cell walls. Wiley, New York

Reiterer A, Jakob HF, Stanzl-Tschegg SE, Fratzl P (1998) Spiral angle of elementary cellulose fibrils in cell walls of *Picea abies* determined by small-angle X-ray scattering. Wood Sci Technol 32:335–345

Schaffer BW (1964) Stress-strain of reinforced plastics parallel and normal to their internal filaments. AIAA J 2:348–352

Spatz H-CH, Köhler L, Speck T (1998) Biomechanics and functional anatomy of hollow-stemmed Sphenopsids. I. *Equisetum giganteum* (Equisetaceae). Am J Bot 85:305–314

Spatz H-CH, Köhler L, Niklas KJ (1999) Mechanical behaviour of plant tissues: composite materials or structures? J Exp Biol 202:3269–3272

Torp S, Arridge RGC, Armeniades CD, Baer E (1975) Structure-property relationship in tendon as a function of age. In: Atkins EDT, Keller A (eds) Structure of fibrous biopolymers. Butterworth, London, pp 197–221

Vincent JFV (1975) Locust oviposition: stress softening of the extensible intersegmental membranes. Proc R Soc London Ser B 188:189–201